

## Turbulent Separated-Reattached Flow around a Blunt Flat Plate

Kamyar Mansour / Department Of Aerospace  
Engineering And New Technologies Research  
Center Amirkabir University of Technology  
Tehran, Iran, 15875-4413

Shirzad Hosseinverdi / Department Of  
Aerospace Engineering, Amirkabir University  
of Technology  
Tehran, Iran, 15875-4413

### ABSTRACT

Turbulent separating-reattaching flow over a flat plate with a blunt leading edge is numerically predicted. Different simulation of flow accomplished to study of the effect of blockage ratio and plate chord to thickness ratio on the flow recirculation and reattachment point for finite and infinite plate. Reynolds number that based on the uniform inlet velocity and plate thickness is  $3.6 \times 10^4$ . Plate chord to thickness ratios varied in a range between 4 and 25 also blockage ratios change between 3% through 40%. The numerical results are compared reasonably well with the both of experimental and numerical data. It is found that reattachment length increases with increases of plate chord to thickness ratio. This increasing is rather large in the case of small chord to thickness ratio and for high chord to thickness ratios the reattachment length is independent of chord to thickness ratio. Reattachment length decreases with the increases of blockage ratio linearly for blockage ratio lower than 25%. Also we calculated the effect of Reynolds number on the flow and reattachment point for only finite plate.

### KEYWORDS:

Blunt flat plate, Turbulent, Separating-Reattaching flow.

### INTRODUCTION

The turbulent separation and reattachment flows are commonly encountered in many engineering problems, both in external flows like flows around airfoils and buildings and in internal flow system such as diffusers, combustors and circular channels with sudden expansion. In these situations, the flow experiences an adverse pressure gradient which causes the flow separate from the solid surface. The flow subsequently reattaches downstream forming a recirculation bubble and the boundary layer develops downstream of the separation point and separation and reattachment of flow may be affected by that. In some applications such as combustors, the presence of the recirculation and turbulence due to separation can help enhance the mixing of fuel and air. On other hand separation in

pipe and duct flow causes loss of available energy. Thus, understanding the flow separation and reattachment phenomena is important in engineering design. The research has been conducted for different geometries such as backward-facing step, forward-facing step, rib, splitter plate and blunt plate. The flow around a flat plate with the leading edge treated in one of the simplest models of a separated and reattached flow. However, the flow structure is very complicated. In two last decades, experimental and theoretical research on the turbulent separated-reattaching flows around the blunt leading edge has been performed in details. Most of these investigations were done for semi-infinite blunt plate. Ota and co-workers [8-10] are pioneers in these studied and summary of the previous studies are reported of Nishiyam [11]. For semi-infinite blunt plates, chord to thickness ratio 25, turbulent measurements in a separated-reattached is made and described by Kiya-Sasaki [1]. The Reynolds number is  $2.6 \times 10^4$  and reattachment found to happen 5.05 times the plate thickness. Cherry et al. [2] measured velocity and surface pressure fluctuations on a blunt plate at a Reynolds number of  $3.2 \times 10^4$  and blockage ratio 3.79%. The reattachment length ( $X_R$ ) is 4.95 times plate thickness Also observed the Reynolds number independent flow regimes. They noted that the flow is essentially Reynolds number independent within the range  $34000 < Re < 80000$ . More recently, Djilali and his co-workers [4-6] performed a series of both numerical and experimental studies of turbulent flow over a bluff rectangular plate. In experiment part, Djilali et al. [5] showed that reattachment length and pressure distribution remained unchanged over Reynolds number range  $2.5 \times 10^4$  to  $9 \times 10^4$  and  $X_R$  equals 4.77 times plate thickness. A few works is done for a finite length plates. Sam et al. [12] measured surface pressure distribution on a body of rectangular cross-section for plate chord to thickness ratio of 6 for both zero angle of attack and various incident angles. An expression is proposed for the reattachment as a function of incident angles. The position of reattachment is less affected by Reynolds number. For zero incidence,  $X_R$  found to happen at  $X_R/D=4.68$ . McCormick et al. [13] have also measured surface pressure distribution and heat

transfer from rectangular prism in cross-flow stream for plate chord to thickness ratio of 4, Reynolds number of  $(2.9-4.9) \times 10^4$  and different angle of attacks. It was showed that reattachment occur about  $X_R/D=3.5$ . Yaghoubi et al [14] performed a series of experiment for finite blunt plates at  $Re=3.6 \times 10^4$  with plate chord to thickness ratios 4, 5, 6 and 9. The reattachment found to at 3.5-4.7 times plate thickness. In fact for finite thick plate the flow was found to be depends on the blunt plate chord to thickness ratio. The purpose of the present study is to numerically predict the turbulent separated and reattached flow at Reynolds number of  $3.6 \times 10^4$  to investigate influence of the blockage and plate chord to thickness ratio upon the velocity fields as compared with experimental and numerical results. The main physical parameters of blunt plate are shown in Fig. 1. The flow separated at the leading edge and then reattaches on the plates surface and subsequently develops in the downstream direction. The flow assumed symmetric respect to the longitudinal axes. The blunt thickness (D) is maintained as constant of 0.02m, and channel height (H) varied to provides a blockage ratio (BR=D/H) of 3% to 40%. Also at the constant blockage ratio of 5%, the blunt chords (C) are 0.08, 0.1, 0.14, 0.18, 0.24, 0.3, 0.4 and 0.5m. This obtained the plate chord to thickness ratios (CR=C/D) of 4 to 25.

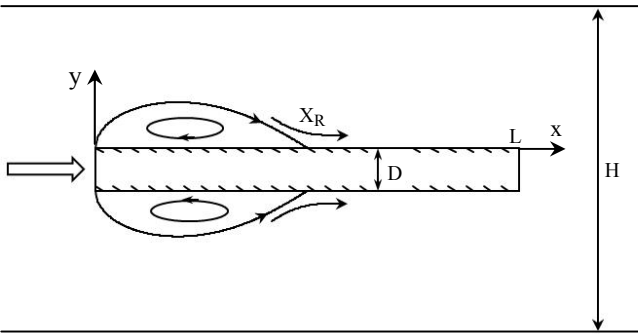


Fig. 1. Blunt flat plate geometry

## 1. GOVERNING EQUATIONS

### 1.1. Reynolds-averaged Navier-Stokes equations

Reynolds-averaged equations For steady, two dimensional and incompressible turbulent flow, for conservation of mass and momentum in conjunction with the isotropic turbulent viscosity hypothesis may be written in a tensor form as follows:

$$\frac{\partial u_i}{\partial x_i} = 0 \quad (1)$$

$$\rho u_j \frac{\partial u_i}{\partial x_j} = -\frac{\partial p}{\partial x_i} + \frac{\partial}{\partial x_j} \left[ 2(\mu_{eff}) S_{ij} - \frac{2}{3} \rho k \delta_{ij} \right] \quad (2)$$

Where

$$\mu_{eff} = \mu + \mu_t \quad (3)$$

$$S_{ij} = \frac{1}{2} \left( \frac{\partial u_i}{\partial x_j} + \frac{\partial u_j}{\partial x_i} \right) \quad (4)$$

### 1.2. Turbulence modeling

In present study, shear-stress transport (SST)  $k-\omega$  of Menter is used as turbulence model, which can give a highly accurate prediction of the onset and the amount of the flow separation under adverse pressure gradient. This model is a two-equation eddy viscosity model which merges the  $K-\omega$  model of Wilcox with a high Reynolds number model  $K-\epsilon$  model (transformed into the  $K-\omega$  formulation). The eddy viscosity is computed through the follow relation

$$\mu_t = \frac{\rho a_1 k}{\max(a_1 \omega, \Omega f_2)} \quad (5)$$

Where  $\Omega$  is the absolute value of the vorticity and  $k$  and  $\omega$  are the turbulent kinetic energy and turbulent specific dissipation that obtained by the solving the follow differential equations.

$$u_j \frac{\partial k}{\partial x_j} = \frac{P_k}{\rho} - \beta^* k \omega + \frac{\partial}{\partial x_j} \left[ (v + \sigma_k v_t) \frac{\partial k}{\partial x_j} \right] \quad (6)$$

$$u_j \frac{\partial \omega}{\partial x_j} = \frac{\alpha P_k}{\mu_t} - \beta \omega^2 + \frac{\partial}{\partial x_j} \left[ (v + \sigma_\omega v_t) \frac{\partial \omega}{\partial x_j} \right] \quad (7)$$

$$+ 2(1 - f_1) \sigma_{\omega 2} \frac{1}{\omega} \frac{\partial k}{\partial x_j} \frac{\partial \omega}{\partial x_j}$$

Turbulent kinetic energy generation,  $p_k$  is defined as

$$P_k = \left[ 2\mu_t S_{ij} - \frac{2}{3} \rho k \delta_{ij} \right] \frac{\partial u_i}{\partial x_j} \quad (8)$$

Auxiliary functions are given by

$$f_2 = \tanh \left[ \left[ \max \left( \frac{2\sqrt{k}}{\beta^* \omega y}, \frac{500\nu}{y^2 \omega} \right) \right]^2 \right] \quad (9)$$

$$f_1 = \tanh(Arg^4) \quad (10)$$

$$Arg = \min \left[ \max \left( \frac{\sqrt{k}}{\beta^* \omega y}, \frac{500\nu}{y^2 \omega} \right), \frac{4\rho \sigma_{\omega 2} k}{CD_{k\omega} y^2} \right] \quad (11)$$

$$CD_{k\omega} = \max \left( 2\rho \sigma_{\omega 2} \frac{1}{\omega} \frac{\partial k}{\partial x_j} \frac{\partial \omega}{\partial x_j}, 10^{-20} \right) \quad (12)$$

where  $y$  stands for the minimum distance to the wall. Model constants are  $a_1=0.31$  and  $\beta^*=0.09$ . The coefficients of  $\alpha$ ,  $\beta$ ,  $\sigma_k$  and  $\sigma_\omega$  are obtained from this relation

$$\phi = f_1\phi_1 + (1 - f_1)\phi_2 \quad (13)$$

Let  $\phi_1$  represent any constant in k- $\omega$  model (inner),  $\phi_2$  any constant in the transformed k- $\epsilon$  model (outer) and  $\phi$  the corresponding constant of k- $\omega$  (SST) model. Constants of inner and outer models are given in table 1.

**Table 1. Inner and outer models constants**

Model	$\alpha$	$\beta$	$\sigma_k$	$\sigma_\omega$
Inner	5/9	3/40	0.85	0.5
Outer	0.44	0.0828	1	0.856

More details and an extensive discussion about the k- $\omega$  (SST) model are reported in [15-16].

### 1.3. Boundary conditions

The boundary conditions applied the computational domain are as follows.

(i) At the inlet, the uniform flow conditions are imposed.

$$u = u_\infty, k = 1.5(Ti \times u_\infty)^2 \text{ and } \omega = k^{3/2} / \lambda H$$

Where  $Ti$  is turbulence intensity,  $\lambda$  is the length scale constant and  $H$  is the channel height.

(ii) At the walls, no-slip boundary conditions are enforced on the wall surfaces.

$$u_w = v_w = k_w = 0 \text{ And } \omega_w = 60\mu / \rho\beta_1\Delta n^2$$

Where  $\Delta n$  denotes the normal distance from the wall.

(iii) At the exit, the zero streamwise gradient is applied because flow is in fully develop condition and exit is far from the recirculation region.

## 2. Numerical procedure and grid independency

The above equations are solved by a finite volume method and non-uniform staggered grid arrangement is used. The convective derivatives are discretized by the QUICK scheme of Hayase et al (1992) and second-order accurate central difference scheme for the rest of spatial derivatives. The resulting finite difference equations are solved numerically by making use of line by line method combined with alternating direction iteration (ADI). SIMPLE algorithm [18] is utilized for the computation of pressure correction in the iteration procedure. The grid highly concentrated to the wall surface and near the blunt plate edge, in order to capture the mean turbulent properties near the wall, that is, there are grid points within  $0 < y^+ < 2$ . Grid independence study was performed using several grid refinement and distribution. Four levels of grid refinement (206(x)×102(y)) is have been used that in every refinement the number of total grid is about 1.2 times and third one selected to be sure of grid independency. The reattachment length was used as the criteria. Predicted velocity profiles at several streamwise

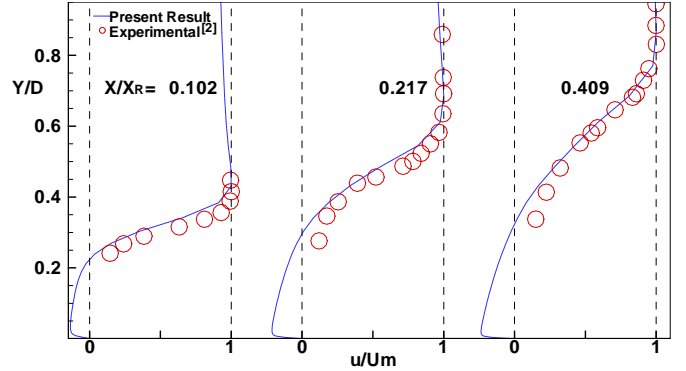


**Fig. 2. Comparisons of the mean velocity profiles with the measurement data at BR=3.79%3.**

locations are compared with measure [2] as shown in Fig .2 with good agreement between predicted measured data. The predicted reattachment length ( $X_R/D$ ) is 5 and it is in excellent agreement with the measured value of 4.95 by Cherry [2].

## 3. Results and Discussion

In numerical simulations of the separated and reattaching flows, the flow reattachment length is the most fundamental quantity that is defined as the point at which the skin friction coefficient changes its sign from negative to positive. We investigate the effect of blockage ratio, blunt plate chord to thickness ratio and Reynolds number on the flow field and reattachment length.

### 3.1 Blockage ratio effect on flow development

The vital factor that has a significant effect on the structure of the flow field is a blockage ratio. Researchers did not pay enough attention to it and more of them hold this ratio constant in their works. for the investigate of this effect, first we investigate the velocity and pressure field for various BR ratios then investigate the effect of them on the variation of reattachment length. The Reynolds number and blunt plate chord to thickness ratio are constant and equal with  $Re=3.6 \times 10^4$  and  $CR=25$ . Fig. 3 shows the mean streamwise velocity over the blunt plate at various station and different BR ratios. The mean velocity is normalized by the local maximum value,  $U_m$  also the y coordinate is normalized by the thickness of boundary layer ( $\delta$ ) where the  $u=0.99U_m$ . Close the leading edge ( $x/d=3$ ) it is seen that lower BR ratios have a large backflow velocities however larger BR ratios do not have a backflow. The same trend seen to continue further downstream, in the recovery region profiles show a an inflexion point as a results of the mergin of new boundary layer with reattaching shear layer , and there is a rapid increase of the near wall velocity with downstream distance. It is seen that for larger blockage ratio flow development is more. These descriptions indicate a more rapid growth of the separation shear layer for larger blockage ratios. The plate wall pressure coefficient is shown in Fig. 4 for different blockage ratios. There is a slight pressure reduction at the leading edge due to flow acceleration and increases in the recirculating zone. Pressure reduction continues

as the fluid flows through the duct. As seen in Fig. 3, larger BR ratios lead to lower recovery pressure. This trend is not surprising since larger blockage ratios should lead to decreases inviscid pressure coefficient according the follow relation.

$$C_{P,Inviscid} = 1 - \left( \frac{U}{U_\infty} \right)^2 = 1 - \left( \frac{H/2}{(H-D)/2} \right)^2 \quad (14)$$

$$C_{P,Inviscid} = 1 - \frac{1}{(1-BR)^2} \quad (15)$$

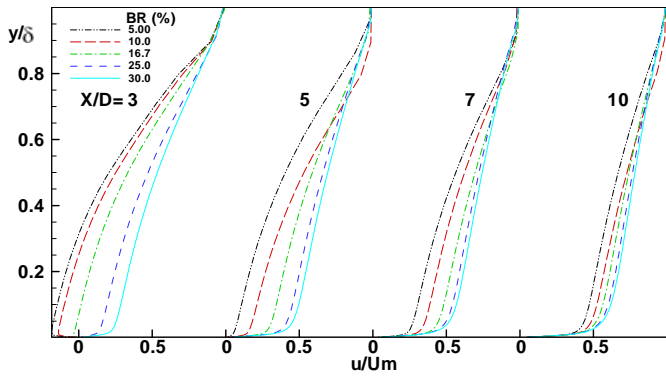


Fig. 3. Mean velocity profile for different BR ratios at various stations at  $Re=3.6 \times 10^4$  and  $CR=25$

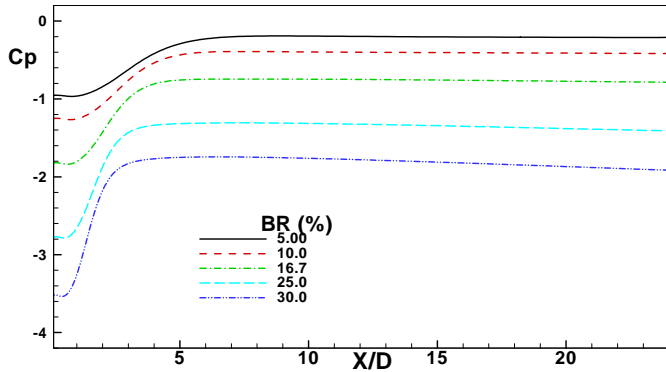


Fig. 4. Variation of surface blunt plate pressure coefficient with blockage ratio

However the Kuehn (1980) showed for the backward facing step that the turbulent separated shear layer prevents the existence of a simple functionality between the pressure coefficient and expansion ratio (the ratio of downstream channel height to upstream channel height). Also at larger BR ratios, the recovery of pressure is occurred at lower distant from the leading edge. Another trend that is evident in the pressure coefficient figure is that larger blockage ratios lead to faster evolution of pressure with shorter distance from the leading edge to the location of minimum pressure coefficient. This can be attributed to the increased flow development rate with larger BR ratios, as evidenced in the velocity field. One important

mechanism, that is known to influence the velocity fields in such a flow, is the mean streamwise pressure gradient,  $dC_p/d(x/d)$ , (averaged over the distance both from the leading to  $x/d=6$  and from minimum  $C_p$  location to  $x/d=6$ ) that increase with increase of blockage ratios. As presented above, the velocity and pressure fields indicate that the larger BR ratios lead to faster growth rates of the separated shear layer downstream of the blunt plate. As a next step, the possible effects of this increased flow development rate on the flow reattachment were investigated. The variation of the reattachment length versus blockage ratio is presented in Fig. 5. The reattachment length is seen to decrease with increasing blockage ratio. This result seems to agree with the velocity field in the following sense. Increasing blockage ratio lead to faster growth rate of the shear layer. Therefore, at larger BR ratios, the separated layer must join the plate wall at the shorter distance from the leading edge. This in turn should result in smaller reattachment length. Also for blockage ratio lower than 25, it is exist a linear function between the BR and  $X_R/d$ .

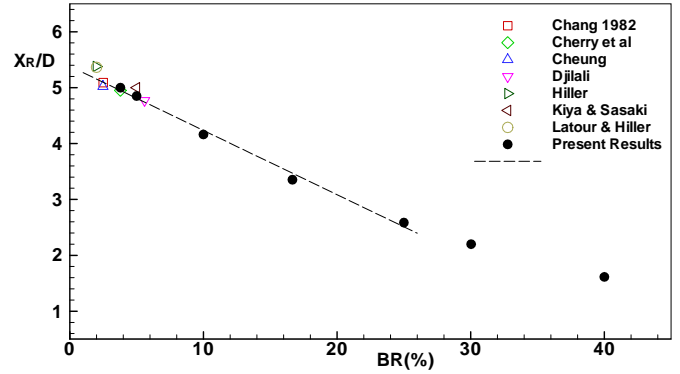


Fig. 5. Variation of reattachment length with blockage ratio at  $Re=3.6 \times 10^4$  and  $CR=25$

### 3.2 Effect of blunt Plate chord to thickness ratio

Second parameter that analyzed in this work is blunt plate chord to thickness ratio (CR). This effect did not reported in studies of researchers. As said in introduction part, the more work in this geometry is done for semi-infinite blunt plate, but this ratio effects on the flow field and reattachment length. The effects of this ratio on the streamwise mean velocity profile at different stations is shown in Fig. 6 at constant blockage ratio ( $BR=5\%$ ) and  $Re=3.6 \times 10^4$ . At small CR ratios the mean velocity profiles are more developed, and for larger CR ratios, there is no different between velocity profiles. These results show that flow development rate decreases with increase of blunt plate chord to thickness ratio. Variation of the reattachment length versus the CR ratio is shown in Fig. 7. The reattachment length increase with increase of plate chord to thickness ratio, but this increment is rather large for small CR ratios, and for larger CR ratios, it is found that the reattachment length independent of CR ratio for  $CR > 12$ . This can attributed to the increase of velocity development rate for small value of CR ratios that lead to the separated shear layer join the blunt plate wall at shorter distance from leading edge. For CR ratios

larger than 12, that the flow development rate does not change, so the reattachment length stayed without change.

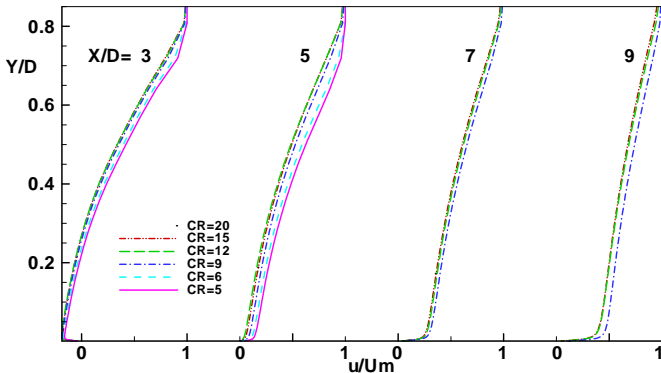


Fig. 6. Mean velocity profile for different CR ratios at various locations at  $Re=3.6 \times 10^4$  and  $BR=5\%$

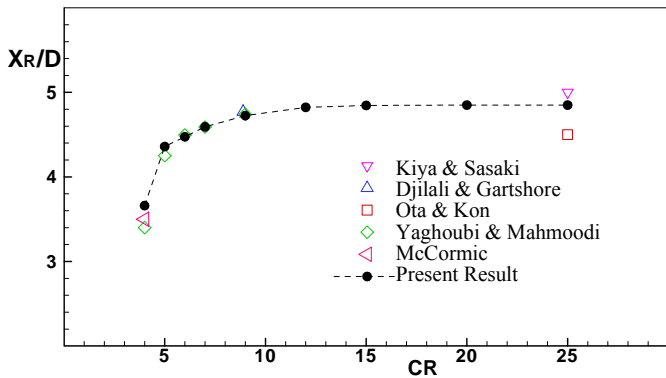


Fig. 7. Variation of reattachment length with blunt plate chord to thickness ratio at  $Re=3.6 \times 10^4$  and  $BR=5\%$

### 3.3 Effect of Re Number on reattachment length

We studied the effect of Reynolds number on reattachment length by using the Re-Normalization Group (RNG)  $k-\epsilon$  turbulence model by Yakhot et al [17] just to see how the length of reattachment varies as Reynolds number increases. In Fig. 8 as can be seen for the case of finite plate with  $CR=9$  and  $BR=5\%$ . It is found that the reattachment length stayed constant

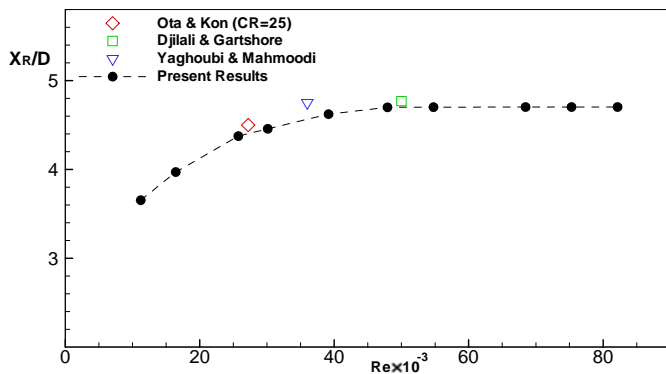


Fig. 8. Variation of reattachment length versus Reynolds Number at  $CR$  equal 9 and  $BR=5\%$ .

For Reynolds Number larger than of about  $3 \times 10^4$  that confirming the observation of Djilali and Gartshore that the reattachment length remained unchanged over the Reynolds number range  $2.5 \times 10^4$  to  $9.0 \times 10^4$ .

## 4. CONCLUSION

Numerical simulations of a separated and reattached flow around a blunt flat plate in a channel are reported at  $Re=3.6 \times 10^4$  in two-dimensional turbulent flow. Based on this analysis the following conclusion can be made.

1. Results indicate that larger blockage ratios lead to faster growth rates of separated shear layer and velocity development before the flow reattaches. As a consequence of this, smaller normalized reattachment lengths ( $X_R/D$ ) are obtained for larger blockage ratios.
2. At constant blockage ratio ( $BR=5\%$ ) and  $Re=3.6 \times 10^4$ , the growth rate of shear layer becomes more for small CR ratios. So the bubble length increases with the increase of CR ratio. The length of separation bubble formed on the plate becomes independent of the blunt chord to thickness ratio that larger than 12 ( $CR>12$ ).
3. For finite blunt plate of  $CR=9$  and  $BR=5\%$ , it is found that reattachment length stayed constant for Reynolds number larger than about  $3 \times 10^4$ .

## NOMENCLATURE

C	Blunt plate chord, m
$C_p$	Pressure coefficient $(p-p_\infty)/0.5\rho U_\infty^2$
D	Blunt thickness, m
H	Channel height, m
k	Turbulent kinetic energy
$U_i$	Velocity component, m/s
$U_\infty$	Free stream velocity
$X_R$	Reattachment length, m

### Greek Symbols

$\mu$	Dynamic viscosity, Pa.s
$\mu_T$	Turbulent viscosity, Pa.s
$\rho$	Mass density, $kg/m^3$
$\omega$	Turbulent specific dissipation

### Subscripts

t	Turbulent
R	Reattachment
$\infty$	Free stream value

### Ratios

CR	Blunt plate chord to thickness ratio, $[C/D]$
BR	Blockage ratio, $[D/H]$
Re	Reynolds number, $[U_\infty D/\nu]$

## REFERENCES

- [1] Kiya M, Sasaki K. Structure of a turbulent separation bubble. J. Fluid Mech 1983;137:83-113

- [2] Cherry NJ, Hillier R, Latour MEP. Unsteady Measurements in a Separated and Reattaching Flows. *J. Fluid Mech* 1984;144:13-46
- [3] Latour MEMP., Hiller R. Experiments on a two-dimensional separated flow. *IC Aero* 1980;TN:80-101.
- [4] Djilali N, Gratshore IS, Salcudean M. Calculation of convective heat transfer in recirculating turbulent flow using various near-wall turbulence models. *Numerical Heat Transfer, part A* 1989;16:189-212
- [5] Djilali N, Gratshore IS. Turbulent flow around a bluff rectangular plate. part I : Experimental Investigation. *ASME J. Fluids Eng* 1991;113:51-59
- [6] Djilali N, Gratshore IS. Turbulent flow around a bluff rectangular plate. part II : numerical predictions. *ASME J. Fluids Eng* 1991;113:60-67
- [7] Tafti DkA, Vanaka SP. A numerical study of flow separation and reattachment on a blunt Plate. *Phys. Fluids A* 1991;3(7):1749-1759
- [8] Ota T, Itsaka M. A separated and reattached flow over a blunt flat plate," *ASME J. Fluids Eng* 1976;98: 79-86
- [9] Ota T, Kon M. Turbulent transfer of momentum and heat in a separated and reattached flow over a blunt flat plate. *ASME Trans. J. Heat Transfer* 1980;96: 459-462
- [10] Ota T, Kon M. Heat transfer in the separation and reattached flow on a blunt flat plate. *Trans, ASME J. Heat Transfer* 1974;96: 459-462
- [11] Ota T., Nishiyama H. A correlation of maximum turbulent heat transfer coefficient in reattachment flow region. *Int. J. Heat Mass Transfer* 1987;30: 1193-1200
- [12] Sam GR, Lessman RG, Test FL. An experimental study of flow over a rectangular body. *ASME Trans. J. Fluid Eng* 1979;101:443-448
- [13] McCormick DC, Lessman RG, Test FL. Heat transfer to separated flow regions from a rectangular prism in a cross stream. *ASME Trans. J. Heat Transfer* 1984;106:276-283
- [14] Yaghoubi M, Mahmoodi S. Experimental study of turbulent separated and reattached flow over a finite blunt plate. *Thermal and Fluid Science* 2004;29:105-112
- [15] Menter FR. Zonal Two Equation  $k-\omega$  Turbulence Models for Aerodynamic Flows. *AIAA Paper* 1993; 93-2906.
- [16] Menter FR. Two-Equation Eddy-Viscosity Turbulence Models for Engineering Applications. *AIAA Journal* 1994; 32: 269-289.
- [17] Yakhot V, Orszag SA, Thangam S, Gatski TB, Speziale, CG. Development of turbulence models for shear flows by a double expansion technique. *Physics of Fluids A* 1992;4: 1510-1520.
- [18] Patankar SV, Spalding DB. A calculation procedure for heat, mass and momentum transfer in three-dimensional parabolic flows. *Int. J. Heat Mass Transfer* 1972;15:1787-1806.